Redesigning an Antibody Fragment for Faster Association with Its Antigen

Jonathan S. Marvin and Henry B. Lowman*

Genentech, Inc., Department of Protein Engineering, South San Francisco, California 94080

Received October 3, 2002; Revised Manuscript Received March 21, 2003

ABSTRACT: Traditional approaches for increasing the affinity of protein−protein complexes focus on constructing highly complementary binding surfaces. Recent theoretical simulations and experimental results suggest that electrostatic steering forces can also be manipulated to increase association rates while leaving dissociation rates unchanged, thus increasing affinity. Here we demonstrate that electrostatic attraction can be enhanced between an antibody fragment and its cognate antigen through application of a few simple rules to identify potential on-rate amplification sites that lie at the periphery of the antigen−antibody interface.

The use of antibody-based therapeutics for the treatment of human diseases (*1*, *2*) has brought about an increased focus on the generation of antibodies to novel targets (*3*) and the molecular details of their interactions (*4*). Typically, development of an efficient and potent antibody involves the identification of a murine monoclonal antibody to the target antigen followed by "humanization" and affinity maturation of the antibody through site-directed mutagenesis, phage display, or other techniques (*5*−*8*). These methods focus on increasing the stereochemical complementarity between the complementarity determining regions (CDRs)[1] and the antigen and can produce antibodies with affinities in the subnanomolar range.

The affinity of a protein−ligand pair is described by the dissociation constant (K_d) and defined as the equilibrium distribution of unbound molecules to bound molecules in solution (eq 1). This relationship can also be defined by the ratio of the dissociation rate (off-rate, k_{-1}) to the association rate (on-rate, k_1). Increases in affinity, which could increase the potency of a therapeutic antibody, can thus be achieved by decreasing the dissociation rate or increasing the association rate. For example, the monovalent antigen-binding fragment of an antibody (P) interacts with antigen (L) according to the following relationship:

$$\mathrm{P} + \mathrm{L} \underset{k_{-1}}{\overset{k_1}{\rightleftharpoons}} \mathrm{PL} \quad K_d = \frac{[\mathrm{P}][\mathrm{L}]}{[\mathrm{PL}]} = \frac{k_{-1}}{k_1} \tag{1}$$

Interestingly, affinity differences among mutants of many proteins (*9*), including the anti-VEGF recombinant human antibody Y0101 (*8*) used in the work reported here, are defined primarily by differences in their dissociation rates. This observation is consistent with the notion that most mutations that increase affinity improve the complementarity of the antibody for the antigen, and that dissociation rates or off-rates (k_{-1}) are dependent on the breaking of short-range interactions (*10*). In contrast, association rates or on-rates (k_1) are dependent on the frequency of collision between the two molecules, and the efficiency with which each collision proceeds to formation of a complex. The latter in turn is dependent on the population of molecules with sufficient thermal activation energy (*11*), as defined by (eq 2):

$$k_1 = \frac{k_B T}{h} e^{-\Delta G^{\ddagger}/RT} \tag{2}$$

where $\Delta G^{\ddagger}$ is the free energy of the transition state, R is the universal gas constant, T is the temperature, k_B is Boltzmann's constant, and h is Planck's constant.

In theory, it is possible to increase the association rate through mutations that increase the efficiency of collision. This can be achieved, without disrupting the short-range contacts that comprise the binding interface, by mutating residues at the periphery of the binding interface to generate favorable electrostatic steering forces (*12*−*15*). Analysis of electrostatically steered associations has proceeded from static computations (*16*, *17*) to solution of the Poisson−Boltzmann equation for use in Brownian dynamics simulations (*18*). It has recently been shown that electrostatic energies of interaction calculated assuming a homogeneous dielectric constant of 80 can predict the relative change in association rate resulting from mutation for a number of protein−protein interactions, including the barnase−barstar complex (*13*, *19*), TEM−lactamase−BLIP inhibitor complex (*15*), acethylcholinesterase−fasciculin complex (*14*), and the hirudin−thrombin complex (*20*, *21*).

Here we demonstrate that the principles of electrostatic attraction can be similarly applied to antibody engineering by increasing the association rate between the antigen-binding fragment (Fab) of a previously humanized antibody (*8*, *22*, *23*) and its cognate antigen. In this case, the antibody Y0101 blocks the activity of vascular endothelial growth factor (VEGF), which initiates blood vessel prolifera-

[1] Abbreviations: Fab, antigen binding antibody fragment; VEGF, vascular endothelial growth factor; CDR, complementarity determining region; ON-RAMPS, on-rate amplification sites; SPR, surface plasmon resonance; SASA, solvent accessible surface area.

10.1021/bi026947q CCC: $25.00
Published on Web 05/17/2003

tion and whose uncontrolled function contributes to many diseases, including cancer (*24*). We identified potential on-rate amplification sites (ON-RAMPS) on the surface of the Fab by applying a series of simple criteria (vide infra). Antibody fragments with mutations made at these candidate sites show association rates increased by nearly an order of magnitude in low ionic-strength solution as determined by a fluorescence-based assay. The association rates observed for the Fab−VEGF complex show limited correlation with the electrostatic energy of interaction as calculated by the method of Schreiber and co-workers (*15*, *25*, *26*). We postulate reasons for this poor correlation and the overall lower magnitude of on-rate enhancement in the Y0101−VEGF system relative to examples cited in the literature.

EXPERIMENTAL PROCEDURES

Identification of On-Rate Amplification Sites (ON-RAMPS). ON-RAMPS were identified using the criteria listed below to reduce the total number of mutatable residues in the anti-VEGF Fab from 437 to an experimentally tractable number.

(i) The residue must have at least one-third of its side chain surface area exposed to solvent, as mutation of buried residues may destabilize the Fab. Using a less stringent value (e.g., 20% exposed) results in the selection of residues that are, by inspection of the structure, too buried; using a more stringent value (e.g., 50% exposed) results in the elimination of residues that are, by inspection, good candidates. However, other systems may require a more stringent criterion to reduce the number of potential ON-RAMPS to an experimentally tractable number.

(ii) The residue must be within at least 16 Å of the antigen in the bound state, as electrostatic attractive forces decay as a function of distance (see eq 3, below). In a theoretical system (at 25 °C in 25 mM Tris·Cl) with a single $-1e$ charge on the antigen, and no charges on the antibody, introducing a $+1e$ charge on the antibody 16 Å from the $-1e$ charge on the antigen would increase the association rate by 15% (if separated by 19 Å, the association rate could increase by 10%).

(iii) The residue must not directly contact the antigen in the bound state, as mutation of direct contact residues may destabilize the bound complex.

(iv) Preference is given to those residues that are within the complementarity determining regions (CDRs) over those that are not, as the hypervariable loops may be less likely to induce immunogenic responses in patients (*6*).

(v) Only those residues for which it is possible to increase the charge complementarity between the Fab and the antigen are considered. For example, V_L-D28 of Y0101 can be mutated to either neutralize (D28N) or reverse (D28K) its charge to better complement the negatively charged antigen, whereas residue V_H-K64 cannot be mutated to increase its positive charge.

Calculation of the Effects of Mutation at ON-RAMPS. The utility of these criteria for the identification of ON-RAMPS was validated by calculating the electrostatic interaction energy and subsequently predicting the on-rate between VEGF and each of 437 "mutant" Fabs, based on the crystal structure of the complex (PDB accession number 1bj1 (*23*)). Importantly, the N-terminal six residues of VEGF (residues 8−13, GQNHHE) are not resolved in this structure. These mutants were generated by replacing the charge on the wild-type residue ($-1e$, $0e$, or $1e$) with a $+1e$ or $-1e$ charge on the C_β atom, using the following equations from the work of Schreiber and co-workers (*15*):

$$U = \sum_{i,j} N_A \frac{q_{a_i} q_{b_j}}{4\pi\epsilon_0 \epsilon r_{a_i b_j}} \cdot \frac{e^{-\kappa(r_{a_i b_j} - a)}}{1 + \kappa a} \quad (3)$$

$$\ln k_{on_{(mut)}} = \frac{U_{wt} - U_{mut}}{0.9} + \ln k_{on_{(wt)}} \quad (4)$$

where N_A is Avogadro's number, q is the charge (in Coulombs, $1e = 1.6 \times 10^{-19}$ C) on atoms i and j within molecules a and b, r is the distance between them (in Angstroms), ϵ is the homogeneous dielectric constant (set to 80 in this work), ϵ_0 is the dielectric constant of a vacuum (8.854×10^{-22} C^2 Å^{-1} J^{-1}), κ is the Debye−Huckel screening parameter that relates ionic-strength (I) to electrostatic shielding (*27*), and a is the minimum separation (Angstroms) of the two molecules in the approximation of the transition state (*13*). The value of κ used in these calculations was 0.0488 ($I = 0.025$). We used an a value of 6 Å, which has been determined previously to provide a good correlation between calculated and observed values for k_{on}(mutant)/k_{on}(wt) (*15*, *25*, *26*).

In calculating U for the "rotamer model" (vide infra), the most favorable rotamer of each mutant residue was determined using the Insight 2000 molecular modeling program (Accelerys), and the energy of interaction calculated as above.

Mutagenesis, Protein Expression, and Purification. The short isoform of VEGF (8−109) was produced as described previously (*28*). The methods for constructing and purifying mutant variants of the Fab have been described previously (*23*). Briefly, point mutations were made by oligonucleotide directed mutagenesis (*29*). The Fab is expressed upon induction in the nonsuppressor *Escherichia coli* cell line 34B8 (*7*) and purified by affinity chromatography with protein G resin (Amersham) after osmotic shock of harvested cells. Typical yields were 0.1 mg (2 nmol) Fab per 1 L growth.

Association Rate Assay. In the experiments described here, the fluorescence emission intensity ($\lambda_{excitation} = 295$ nm; $\lambda_{emission} = 340$ nm, 16 nm band-pass) was measured using an 8000-series SLM-Aminco spectrophotometer (Thermo-Spectronic). VEGF was added to a stirred cuvette containing approximately 10 nM Fab in 25 mM Tris, pH 7.2, at 37 °C.

Dissociation Rate Assay. Dissociation rates were measured by surface plasmon resonance on a BIAcore-2000 or -3000 instrument (BIAcore, Inc.) as described previously (*23*), as the dissociation rates are too slow to be accurately measured by the fluorescence-based assay. VEGF was immobilized by amine coupling to a CM5 chip at final densities of approximately 16, 45, and 90 resonance-response units. Fab binding was measured with sample concentrations of 1 μM, 500 nM, 250 nM, 125 nM. The dissociation constant was calculated assuming a one-to-one binding model, and standard deviations determined from these 12 binding curves. Experiments were performed at 37 °C in 25 mM Tris, pH 7.2, 0.01% NaN_3, or at 25 °C in 25 mM Tris, 0.15 M NaCl, 0.01% NaN_3. The flow rate was set to 20 μL min^{-1}.

RESULTS

Development of the Association Rate Assay. An accurate method for determining association rates is essential to any effort to enhance them. While surface plasmon resonance technology is suitable for affinity measurements, subtle differences in association rates among variants of a protein may go unnoticed for multiple reasons, ranging from the complexities of flow-dynamics (*30*) and nonspecific amine coupling (*31*) to inaccuracies in the determination of concentrations of properly folded and active proteins.

Since the work presented here is concerned with differences in binding rates among variants of the anti-VEGF Fab, it was necessary to develop an assay that is representative of the interaction in solution, sensitive enough to detect subtle differences in on-rates, and independent of the concentration of various Fab variants. This latter requirement precludes the interpretation of differences that may result from inaccurately determined Fab concentrations as differences in the intrinsic on-rate (k_1).

We chose to use intrinsic fluorescence as a means to assay unmodified antibody interactions with antigen. The fluorescence properties of tryptophan residues are sensitive to their local environment (*32*). As revealed by the co-structure of VEGF with Y0101 (*23*), there are three tryptophans in the Fab that form direct contacts with VEGF in the bound state and whose fluorescence properties might be expected to change upon binding. There are no tryptophans in VEGF, but there are two tyrosines and one phenylalanine that form part of the binding interface with the Fab (*23*). These might also contribute to the fluorescence spectrum if excited. To circumvent this potential source of error, the fluorescence assay was performed with an excitation wavelength of 295 nm, which minimally overlaps with the excitation spectra of tyrosine and phenylalanine (*32*).

We first determined that the fluorescence intensity of the Y0101−VEGF complex is greater than the sum of the individual fluorescence intensities of the components (Figure 1a). Furthermore, when Fab and VEGF are mixed, the rate of increase of the fluorescence intensity can be recorded and fit to a single-exponential curve (Figure 1b). Plotting the observed rate as a function of VEGF concentration permits pseudo-first-order analysis, the slope being k_1 for the reaction (*33*) (Figure 1c).

Identification of ON-RAMPS. Fab Y0101 has 445 residues, 437 of which are resolved in the structure of its complex with VEGF (*23*). Attempting to improve the affinity of an antibody by mutating residues that lie *outside the binding interface* would be overwhelming if each residue were considered individually. We have thus developed an algorithm for reducing the list of all noncontact residues to a significantly smaller number that can be inspected on an individual basis (see Experimental Procedures). This process eliminated residues that are greater than 16 Å away from the antigen and avoids framework residues, reducing the number of potential sites for mutagenesis from 437 residues to 20 (Table 1).

The first criterion, being solvent exposed, reduces the number to 173. The second, being within 16 Å of VEGF, reduces the number to 47. The third, not directly contacting VEGF, reduces the number to 31. The fourth, that the residue lie within the CDRs, reduces that to 21. Finally, one additional residue (V_H-K64) is eliminated by the final criterion, as its complementarity with the negatively charged VEGF cannot be increased. The predicted on-rate for mutation of each of these residues to a positively charged residue was calculated according to the method of Schreiber and co-workers (*15*).

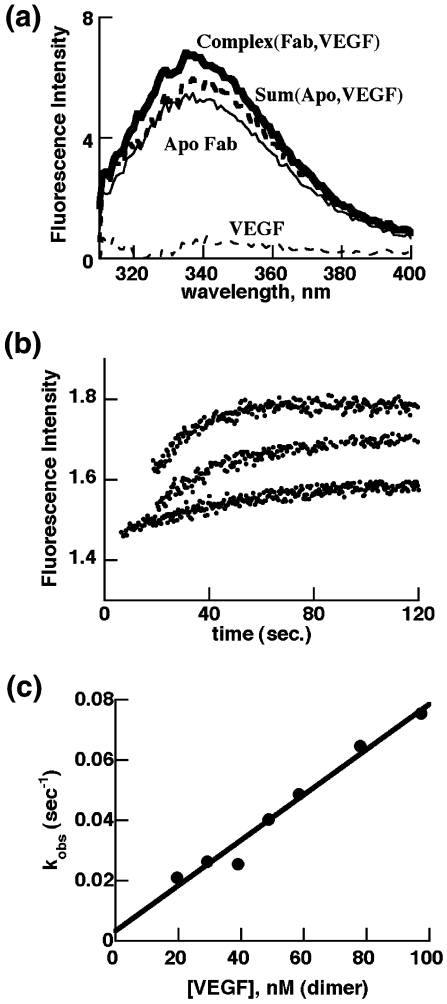

FIGURE 1: (a) The emission spectrum of a mixture of 10 nM Fab with 120 nM VEGF (thick, solid) is greater than the sum (thick, dashed) of the individual spectra of ~10 nM Fab Y0101 (thin, solid) and ~120 nM VEGF (thin, dashed). (b) The rate of formation of the complex (ΔFluorescence) can be measured as a function of time with varying concentrations of VEGF (increasing in concentration from bottom to top) and fit to a single exponential to determine the observed rate (k_{obs}). (c) Plotting the observed rate of formation of the complex (k_{obs}) against the concentration of VEGF used permits pseudo-first-order analysis to determine k_1, given by the slope of the plot. The data shown here are for the heavy chain mutant T28E, at 3.9 nM.

Observed Association Rates. Since the net formal charge on a molecule of VEGF is $-10e$ (calculated by assigning $+1e$ to the N-termini, lysines, and arginines, and $-1e$ to the C-termini, aspartates and glutamates; no charge was assigned to any of the histidines; the NMR structure of VEGF indicates that none of them are doubly protonated (*34*)), and mutations were made to increase the net positive charge on the Fab (wild-type = $+2e$) at the periphery of the binding interface. Mutation of these residues results in increases in association rate as great as 2-fold relative to Y0101 (Table 2). On the other hand, mutations of residues that are solvent exposed, but not within 16 Å of VEGF (Table 2, unqualified),

Table 1: Potential ON-RAMPS[a]

residue	% SASA	minimum distance from VEGF (Å)	calculated on-rate (relative to wt)
		Light Chain	
Ser 26	38	15.7	1.2
Gln 27	58	11.8	1.1
Asp 28	66	13.4	1.4
Ser 30	50	11.2	1.3
Asn 31	44	12.5	1.2
Tyr 32	48	6.3	1.1
Phe 50	43	9.7	1.2
Ser 52	60	15.3	1.2
Ser 53	42	10.4	1.2
Leu 54	37	13.9	1.1
Ser 56	90	10.5	1.1
Thr 93	56	6.9	1.1
Val 94	34	3.9	1.1
		Heavy Chain	
Ser 25	54	15.1	1.1
Thr 28	69	6.4	1.1
Thr 30	36	5.9	1.2
Thr 54	36	4.4	1.2
Glu 56	80	6.5	1.6
Ala 61	93	11.4	1.1
Asp 62	87	15.3	1.1
Tyr 99	84	3.5	1.6
Ser 100a	68	4.9	1.3

[a] Residues are numbered according to the the Kabat system (*37*). %SASA calculated using a 1.4 Å probe radius.

Table 2: Binding Constants of Single Mutations[a]

mutation	k_1 ($\times 10^5$ M^{-1} s^{-1})	k_{-1} ($\times 10^{-4}$ s^{-1}) 0 M NaCl	k_{-1} ($\times 10^{-4}$ s^{-1}) 0.15 M NaCl	K_d ($\times 10^{-9}$ M)
Y0101 (wild-type)	5.4 ± 0.3	3.9 ± 1.1	1.3 ± 0.5	0.7
		Light Chain		
R18Q[b]	4.8	3.8 ± 0.5	0.9 ± 0.3	0.8
R18E[b]	5.2	2.6 ± 0.7	0.9 ± 0.2	0.5
S26K	7.4	3.3 ± 0.5	0.6 ± 0.3	0.4
Q27K	6.7	4.0 ± 0.4	0.7 ± 0.4	0.6
D28K	7.0	3.3 ± 0.2	0.9 ± 0.4	0.5
D28N	6.5	2.8 ± 0.8	0.9 ± 0.3	0.4
S30K	9.7	3.3 ±0.5	0.3 ± 0.1	0.3
S30N	5.5	3.3 ± 0.4	0.9 ± 0.3	0.6
N31K	6.9	3.3 ± 0.5	0.3 ± 0.2	0.5
N31R	7.8	3.8 ± 0.2	0.4 ± 0.2	0.5
Y32K	7.3	2.5 ± 0.4	0.4 ± 0.2	0.3
Y32R	7.1	LE[c]	LE	
S52K	6.2	3.8 ± 0.2	0.6 ± 0.2	0.6
S53K	8.0	3.8 ± 0.2	0.5 ± 0.2	0.5
L54K	4.4	LE	LE	
V94E	1.3	10.1 ± 1.0	4.4 ± 0.8	7.8
E195R[b]	4.9	BG[d]	LE	
E195Q[b]	5.9	5.3 ± 2.5	1.5 ± 0.7	0.9
E195L[b]	7.3	BG	0.6 ± 0.2	
		Heavy Chain		
T28K	3.6	LE	LE	
T28R	4.0	4.8 ±0.4	LE	1.2
T28E	7.8	4.8 ± 0.3	1.0 ± 0.1	0.6
T28D	10.	2.9 ± 0.2	0.8 ± 0.3	0.3
T30D	6.0	2.6 ± 1.4	1.0 ± 0.1	0.4
T30E	4.8	7.2 ± 0.3	1.4 ± 0.2	1.5
E56K	4.8	4.4 ± 0.3	LE	0.9
Y99K	3.8	1.5 ±1.2	1.4 ± 0.3	0.4
Y99R	6.0	1.4 ± 1.3	1.6 ± 0.3	0.2
S100aR	8.7	2.4 ± 0.8	0.7 ± 0.1	0.3
D218N[b]	4.9	BG	0.8 ± 0.2	
D218K[b]	5.3	BG	0.6 ± 0.4	

[a] k_1 determined by the fluorescence-based assay (± standard deviation of three experiments, wild-type only). k_{-1} determined by surface plasmon resonance (± standard deviation of 12 experiments (see Methods)). k_1 and k_{-1} (0 M NaCl) experiments were performed in 25 mM Tris, pH 7.2, at 37 °C. k_{-1} (0.15 M NaCl) experiments performed in 25 mM Tris, 150 mM NaCl, at 25 °C. K_d is calculated from 0 M NaCl data. Residues are numbered according to the Kabat system (*37*). [b] Residues that do not meet the ON-RAMPS criteria. [c] LE, low expression of Fab limited analysis. [d] BG, background binding to control flow cell limited analysis of SPR data.

show little change, thus illustrating the utility of the ON-RAMPS criteria. Further increases in the association rate of the anti-VEGF Fab were achieved by mutating multiple residues (Table 3), with the fastest binding variant, "34-TKKT" (V_H-(T28D, S100aR) + V_L-(S26T, Q27K, D28K, S30T)) having an association rate 6-fold higher than that of Y0101. Conversely, mutations that gave rise to charge repulsion resulted in decreased association rates (Table 3: mutant V_L-S26E, Q27E, D28E, S30E, and mutant V_L-T51E, S52E, S53E, L54E).

Salt Dependence of Association Rates. To illustrate that the difference in association rates between variants is attributable to the electrostatic interaction between the Fabs and VEGF, rather than a general structural rearrangement of the binding interface, we measured the association rates of the wild-type Fab Y0101 and 34-TKKT at different salt concentrations (Figure 2). The difference in association rate between the fastest binding variant and Y0101 in 150 mM NaCl at 37 °C is only 2-fold (Y0101, 3.9×10^5 M^{-1} s^{-1}; 34-TKKT, 8.1×10^5 M^{-1} s^{-1}), and the dissociation rates are mostly the same (Y0101, 3.9×10^{-4} s^{-1}; 34-TKKT, 3.3×10^{-4} s^{-1}). The increased ionic strength sensitivity of the association rate of 34-TKKT relative to the insensitivity of the Y0101 association rate is consistent with a contribution from electrostatic steering forces.

Importantly, the electrostatic energy of interaction between the Fab and VEGF as calculated from the structure of the complex (Y0101 = 0.28 kcal mol^{-1}, 34-TKKT = −1.07 kcal mol^{-1}) is of the correct sign (though differing in magnitude) with the value determined from the slope of Figure 2. (Y0101 = 0.86 kcal mol^{-1}, 34-TKKT = −4.0 kcal mol^{-1}).

Comparison of Experimental and Calculated Rates of Association. It has been suggested that the electrostatic interaction energy of a protein−protein complex, calculated using a homogeneous dielectric constant, is a powerful and accurate predictor of association rate (*15*, *25*, *26*). We calculated the electrostatic interaction energy for the different variants constructed in this study by this method using two slightly different models for the distribution of charges within the proteins, assuming one-to-one complex formation (as the dimeric VEGF is in excess).

In the simpler "sequence position model", the distribution of charges was approximated by assigning formal charges to the C_B atoms of Lys, Arg, Asp, and Glu residues, the N-terminal nitrogens, and the C-terminal carboxylate oxygens. For comparison, a "rotamer model" was used in which the side chain of each mutated residue was replaced with the energetically most favorable rotamer and the distribution of charges within the protein approximated by assigning formal charges of $+1e$ to the N_ζ of lysines, and the N-terminal nitrogen, $+0.5e$ to each of the N_η of arginines, $-1e$ to the C-terminal carboxylate oxygen, and $-0.5e$ to each of the carboxylate oxygen atoms of aspartates and glutamates.

Table 3: Binding Constants of Multiple Mutations[a]

mutations	calculated k_1 ($\times 10^5$ M^{-1} s^{-1})	k_1 ($\times 10^5$ M^{-1} s^{-1})	k_{-1} ($\times 10^{-4}$ s^{-1}) 0 M NaCl	k_{-1} ($\times 10^{-4}$ s^{-1}) 0.15 M NaCl	K_d ($\times 10^{-9}$ M)
		Light Chain			
S26E, Q27E, D28E, S30E	3.2	2.6	5.1 ± 0.8	0.8 ± 0.2	2.0
S26K, Q27K, D28N, S30T	9.0	6.1	BG[b]	LE	
S26K, D28K, S30K	12.5	13	LE[c]	LE	
S26K, Q27K, D28N, S30K	12.5	13	BG	0.7 ± 0.1	
S26K, Q27K, D28K, S30T	12.5	21	BG	0.4 ± 0.1	
S26T, Q27K, D28K, S30K	15.7	25 ± 1.0	BG	0.6 ± 0.1	
S26T, Q27K, D28K, S30T	10.3	29 ± 2.9	BG	0.6 ± 0.1	
T51E, S52E, S53E, L54E	2.7	3.3	4.4 ±1.0	40.8 ± 14.7	1.3
S52K, S53K, L54T	8.1	13	BG	LE	
S26K, Q27K, D28K, S30K, T51K, S52K, S53K, L54K	32.4	24	7.8 ± 1.1	0.9 ± 0.2	0.3
		Heavy Chain			
T28D, S100aR	21.6	14	BG	1.1 ± 0.3	
		Fastest Binding Variant			
34-TKKT	38.9	33 ± 3.9	2.6 ± 1.2	0.2 ± 0.1	0.08

[a] Calculated k_1 determined using the C_β model (see Methods). k_1 determined by the fluorescence-based assay (± standard deviation of three experiments). k_{-1} determined by surface plasmon resonance (± standard deviation of 12 experiments (see Methods)). k_1 and k_{-1} (0 M NaCl) experiments were performed in 25 mM Tris, pH 7.2, at 37 °C. k_{-1} (0.15 M NaCl) experiments performed in 25 mM Tris, 150 mM NaCl, at 25 °C. K_d is calculated from 0 M NaCl data. Residues are numbered according to the Kabat system (*37*). 34-TKKT, mutant V_H-(T28, S100aR) + V_L-(S26T,Q27K,D28K,S30T). [b] BG, background binding to control flow cell limited analysis of SPR data. [c] LE, low expression of Fab limited analysis.

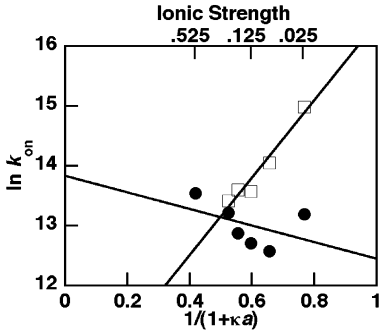

FIGURE 2: Dependence of association rate on ionic strength. The association rate for Y0101 (filled circles) and the fastest binding variant, "34-TKKT" (V_H-(T28D,S100aR) + V_L-(S26T, Q27K, D28K, S30T)) (open squares) was measured as a function of salt concentration. The slopes (−U/RT) are −1.4 and 6.5, respectively, corresponding to U of +0.86 kcal mol^{-1} for Y0101 and −4.0 kcal mol^{-1} for the fastest binding variant.

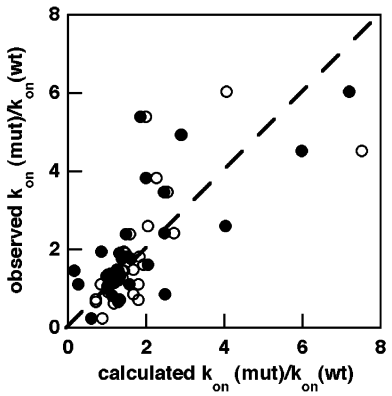

FIGURE 3: Comparison of the observed association rate enhancement (relative to Y0101) with the calculated rate enhancement in the "rotamer model" (filled circles) and the "sequence position model" (empty circles). The dashed line represents a theoretical perfect correlation.

Both methods successfully predict that only minor increases in association rate can occur from individual mutations (with one exception, V_H-T28, see below) and that multiple mutations are required to observe significant increases in this system. However, the correlation is poor for the rotamer model ($R = 0.68$) and worse for the sequence position model ($R = 0.53$), indicating that such a simple method has limited accuracy when applied to a system with low electrostatic potentials (Figure 3).

CONCLUSIONS AND DISCUSSION

The association rates of the several mutants of Y0101 described here are increased by as much as 6-fold relative to the parent Fab and are dependent on ionic strength. The best improvement results from a net increase in the formal charge of light chain CDR-1 by +3*e*, of heavy chain CDR-3 by +1*e*, and by inclusion of the counter-predicted V_H-T28D mutation. None of these mutations are within the direct contact region (Figure 4), reinforcing the idea that improvements in affinity need not result from mutations to the binding interface (*35*). Furthermore, the dissociation rates are mostly unchanged or somewhat improved (Tables 2 and 3), consistent with the expected behavior for an interaction with an increased electrostatic component (*10*). However, the increases in association rate are not nearly as striking as those cited in the literature for other pairs of proteins (e.g., a 1000-fold increase in the association rate of barnase and barstar (*13*)).

The physical basis for the comparatively small differences in the k_{on} values for the variants of Y0101 is revealed by inspection of the structure of the complex (*23*) and analysis of the individual electrostatic interactions between charged atoms in the complex. In the barnase−barstar complex, the closest pair of charged residues at the interface is only 2.5 Å apart, and there are 188 total charge−charge interactions separated by less than 16 Å, while in the Y0101−VEGF complex the closest pair is 7.9 Å apart, and there are only 25 pairs separated by less than 16 Å. Thus, the individual and cumulative effects of each charged residue mutation in Y0101 are significantly less than the effects of each mutation in barnase. If Y0101 bound a different epitope of VEGF, closer to the large patches of negative charge, then we would

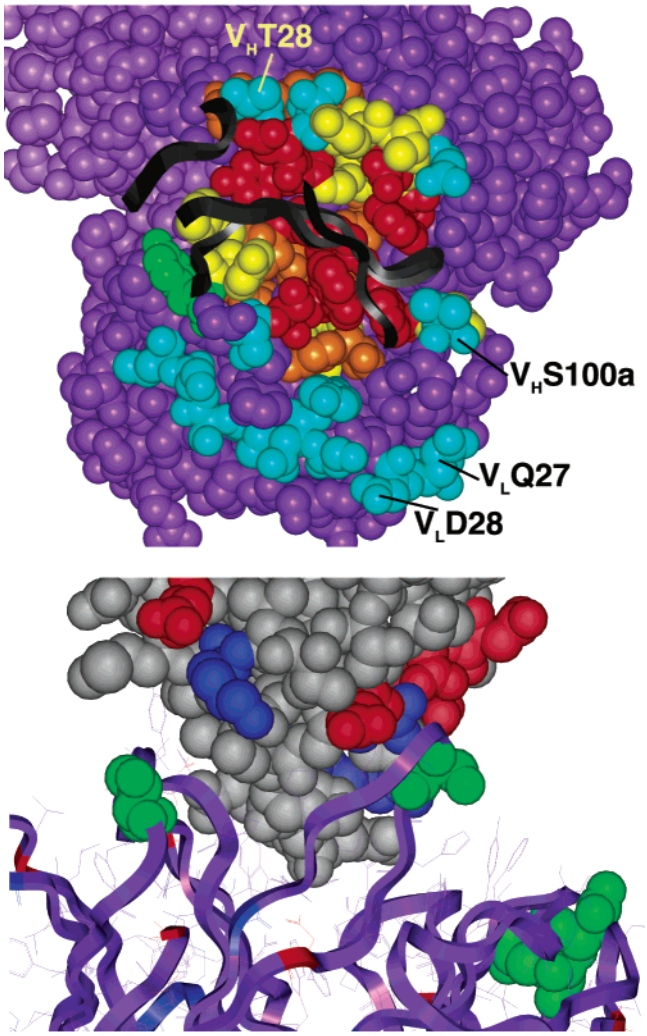

FIGURE 4: (Top) Location of ON-RAMPS. The structure of the complex between Y0101 (CPK rendered) and VEGF (black ribbon), shows that ON-RAMPS (cyan) are located at the periphery of the binding interface. The residues that comprise the binding interface are colored according to their relative contributions to binding, as determined by alanine scanning mutagenesis (*23*). $IC_{50(Ala)}/IC_{50(wt)}$: > 150, red; >10, orange; >3, yellow. V_H-Y99 (green) was also mutated in this study even though the Y99A mutation results in a 4.6-fold loss in affinity. The charge mutations that comprise the fastest binding protein are individually labeled. Adapted from 1bj1 (*23*). (Bottom) Location of the mutations in FabY0101 (purple ribbon and sticks) that comprise the fastest binding protein (CPK rendered, green) in relation to the charged residues (Asp and Glu, red; Arg and lys, blue) of VEGF (grey).

expect the association rate to be more significantly impacted by ON-RAMPS selected using our criteria.

Given the simplicity of the method for calculating the electrostatic energy of interaction, and the absence of charged residues on VEGF at the interface of the complex, the fact that application of the ON-RAMPS criteria successfully increases k_{on} by 6-fold is remarkable. However, while the most significant increases in association rate are predicted to result from mutation of V_H-E56 or V_H-Y99 to positively charged residues (Table 1), the on-rates for these mutants are mostly unchanged from Y0101 (Table 2). The gain in electrostatic energy from mutation of V_H-Y99 to Arg or Lys is expected to be offset by the loss of some van der Waals interactions (Figure 4 and ref *8*), but there is no obvious rationale for the ineffectiveness of the V_H-E56K mutation.

In addition, contrary to both intuition and the predictions of the "rotamer model" of electrostatic interactions (regardless of which rotamer of Asp, Glu, Lys, or Arg is used), the association rate is decreased when residue V_H-T28 is mutated to Lys or Arg and conversely increased when mutated to Asp or Glu. Even calculation based on multiple rotamers did not predict this; however, the simpler "sequence position model" correctly predicts this phenomenon. It is unlikely that the simple model in general more accurately represents the distribution of charges, although it is possible that actual side chain mobility leads to a charge distribution better reflected by the sequence position model than by the rotamer model. Interestingly, mutation of V_H-T28 to Asp or Glu was selected in a phage display affinity maturation study (*8*). It is also possible that the N-terminal six residues of VEGF (and the N-terminus itself) play a role in the kinetics of complex formation, even though they appear to have a minimal role in the overall equilibrium of complex formation, being unresolved in the crystal structures of the Y0101−VEGF complex (*23*), the affinity matured Fab−VEGF complex (*8*), the Flt-1 receptor−VEGF complex (*36*), and an antagonist peptide−VEGF complex (*34*).

In summary, we have demonstrated that the criteria described here for the identification of ON-RAMPS is sufficient for guiding the redesign of an antibody fragment for improved association with its antigen. Although the on-rate for this antibody−antigen pair is enhanced only 6-fold, the increase is significant, and serves as a model system for determining the sensitivity of the method of calculating electrostatic interaction energies from a static structure of the complex. Furthermore, with concomitant improvements in the off-rate, the use of ON-RAMPS results in an improvement in the overall affinity of this antibody by an order of magnitude in the absence of salt (Table 3), and by 2.5-fold in 150 mM NaCl.

ACKNOWLEDGMENT

The authors would like to thank Barbara Moffat for purification of VEGF and the Genentech oligonucleotide synthesis facility.

REFERENCES

1. Fan, Z., and Mendelsohn, J. (1998) *Curr. Opin. Oncol. 10*, 67−73.
2. Gavilondo, J. V., and Larrick, J. W. (2000) *Biotechniques 29*, 128−32.
3. Pardoll, D. M. (2002) *Nat. Rev. Immunol. 2*, 227−38.
4. Eigenbrot, C., Randal, M., Presta, L., Carter, P., and Kossiakoff, A. A. (1993) *J. Mol. Biol. 229*, 969−95.
5. Jones, P. T., Dear, P. H., Foote, J., Neuberger, M. S., and Winter, G. (1986) *Nature 321*, 522−5.
6. Carter, P., Presta, L., Gorman, C. M., Ridgway, J. B., Henner, D., Wong, W. L., Rowland, A. M., Kotts, C., Carver, M. E., and Shepard, H. M. (1992) *Proc. Natl. Acad. Sci. U.S.A. 89*, 4285−9.
7. Baca, M., Presta, L. G., O'Connor, S. J., and Wells, J. A. (1997) *J. Biol. Chem. 272*, 10678−84.
8. Chen, Y., Wiesmann, C., Fuh, G., Li, B., Christinger, H. W., McKay, P., de Vos, A. M., and Lowman, H. B. (1999) *J. Mol. Biol. 293*, 865−81.
9. Voss, E. W. (1993) *J. Mol. Recognit. 6*, 51−8.
10. Zhou, H. X. (2001) *Biopolymers 59*, 427−33.
11. Fersht, A. R. (1985) *Enzyme Structure and Mechanism*, W. H. Freeman and Company, New York.
12. Berg, O. G., and von Hippel, P. H. (1985) *Annu. Rev. Biophys. Bioeng. 14*, 131−60.

13. Schreiber, G., and Fersht, A. R. (1996) *Nat. Struct. Biol. 3*, 427−31.
14. Radic, Z., Kirchhoff, P. D., Quinn, D. M., McCammon, J. A., and Taylor, P. (1997) *J. Biol. Chem. 272*, 23265−77.
15. Selzer, T., Albeck, S., and Schreiber, G. (2000) *Nat. Struct. Biol. 7*, 537−41.
16. Friend, S. H., Matthew, J. B., and Gurd, F. R. (1981) *Biochemistry 20*, 580−6.
17. Matthew, J. B., Weber, P. C., Salemme, F. R., and Richards, F. M. (1983) *Nature 301*, 169−71.
18. Gabdoulline, R. R., and Wade, R. C. (2002) *Curr. Opin. Struct. Biol. 12*, 204−13.
19. Vijayakumar, M., Wong, K. Y., Schreiber, G., Fersht, A. R., Szabo, A., and Zhou, H. X. (1998) *J. Mol. Biol. 278*, 1015−24.
20. Jackman, M. P., Parry, M. A., Hofsteenge, J., and Stone, S. R. (1992) *J. Biol. Chem. 267*, 15375−83.
21. Betz, A., Hofsteenge, J., and Stone, S. R. (1991) *Biochem. J. 275*, 801−3.
22. Kim, K. J., Li, B., Winer, J., Armanini, M., Gillett, N., Phillips, H. S., and Ferrara, N. (1993) *Nature 362*, 841−4.
23. Muller, Y. A., Chen, Y., Christinger, H. W., Li, B., Cunningham, B. C., Lowman, H. B., and de Vos, A. M. (1998) *Structure 6*, 1153−67.
24. Ferrara, N. (1999) *Curr. Top. Microbiol. Immunol. 237*, 1−30.
25. Selzer, T., and Schreiber, G. (1999) *J. Mol. Biol. 287*, 409−19.
26. Selzer, T., and Schreiber, G. (2001) *Proteins 45*, 190−8.
27. Garcia-Moreno, B. (1994) *Methods Enzymol. 240*, 645−67.
28. Christinger, H. W., Muller, Y. A., Berleau, L. T., Keyt, B. A., Cunningham, B. C., Ferrara, N., and de Vos, A. M. (1996) *Proteins 26*, 353−7.
29. Kunkel, T. A. (1985) *Proc. Natl. Acad. Sci. U.S.A. 82*, 488−92.
30. Fivash, M., Towler, E. M., and Fisher, R. J. (1998) *Curr. Opin. Biotechnol. 9*, 97−101.
31. Kortt, A. A., Oddie, G. W., Iliades, P., Gruen, L. C., and Hudson, P. J. (1997) *Anal. Biochem. 253*, 103−11.
32. Lakowicz, J. R. (1999) *Principles of Fluorescence Spectroscopy*, 2nd ed., Kluwer Academic Press, New York, N. Y.
33. Johnson, K. A. (1992) in *The Enzymes* pp 1−61, Academic Press, Inc., New York.
34. Pan, B., Li, B., Russell, S. J., Tom, J. Y., Cochran, A. G., and Fairbrother, W. J. (2002) *J. Mol. Biol. 316*, 769−87.
35. Low, N. M., Holliger, P. H., and Winter, G. (1996) *J. Mol. Biol. 260*, 359−68.
36. Wiesmann, C., Fuh, G., Christinger, H. W., Eigenbrot, C., Wells, J. A., and de Vos, A. M. (1997) *Cell 91*, 695−704.
37. Kabat, E. A., Wu, T. T., Perry, H. M., Gottesman, K. S., and Foeller, C. (1991) *Sequences of Proteins of Immunological Interest*, National Institutes of Health, Bethesda, Maryland.

BI026947Q